GMR
The Original

ECO-FRIENDLY POLYHYDROXYBUTYRATE-CHITOSAN-ZINC NANOCOMPOSITES: A SUSTAINABLE APPROACH TO ANTIMICROBIAL AND SEED GERMINATION APPLICATIONS

Kashish Sharma[1,2], Raunak Dhanker[3], Shivi Choudhary[1,3]*, Sahreen Naseer[2], Sujeeta Yadav[1], Priyanka Sangwan[1], Shivani[2], Sudiksha Pathania[2]

[1]Department of Microbiology, College of Basic Sciences and Humanities, CCS Haryana Agricultural University, Hisar, Haryana-125004, India
[2]University School of Life Sciences, Rayat Bahra University, Mohali, Punjab-140301, India
[3]Department of Basic and Applied Sciences, School of Engineering and Sciences, G. D. Goenka University, Gurugram, Haryana-122102, India
*Corresponding author: 19.choudharyshivi.96@gmail.com

Graphical Abstract

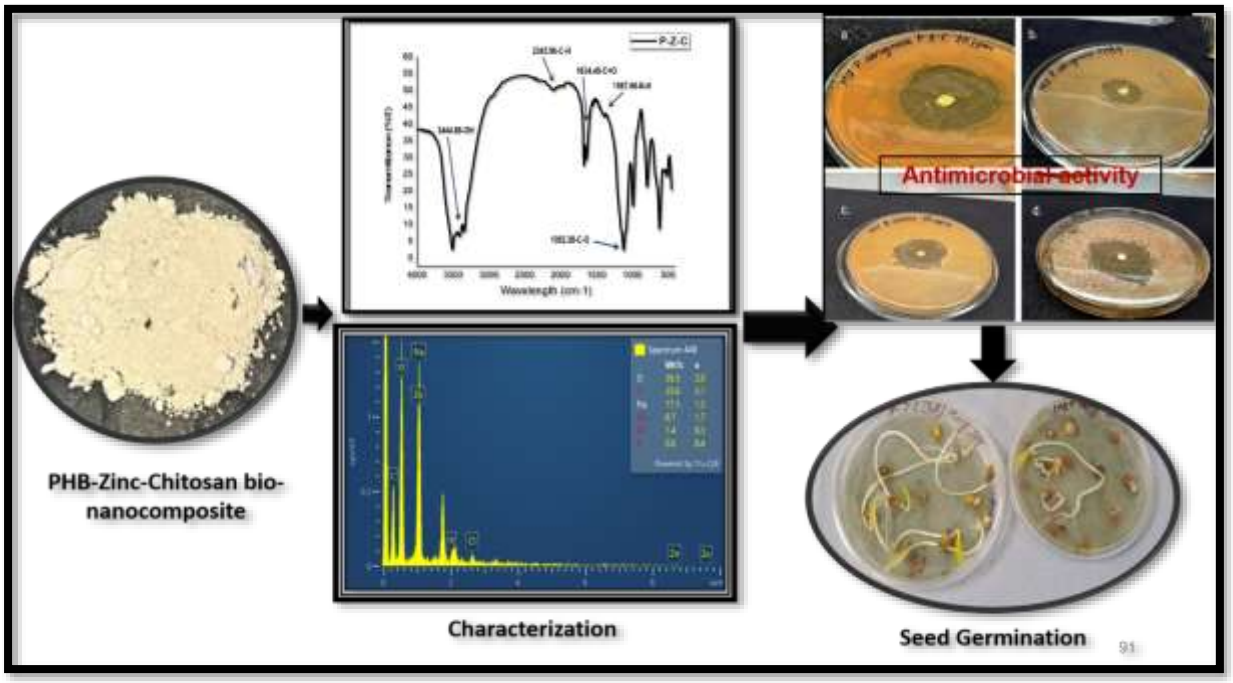

ABSTRACT

Nanoscience has vast promises in the 21st century, especially its revolutionary applications in biotechnology. Of these, bio-nanocomposites represent new materials synthesized by incorporating inorganic nanomaterials in biopolymers to achieve reinforced matrices possessing better mechanical, thermal, and functional properties. This research has examined the synthesis and characterization of a new PHB-Zinc-Chitosan (P-Z-C) bio-nanocomposite synthesized via a simple precipitation approach. The bio-nanocomposite was synthesized by combining polyhydroxybutyrate (PHB) with zinc oxide and chitosan nanoparticles. FTIR, PSA, XRD, and FE-SEM characterization techniques verified the presence of principal functional groups, nanometer particle size (104.1 nm), crystallinity behavior, and porous surface morphology with incorporated zinc clusters. EDX analysis verified the elemental analysis, which was marked with higher carbon, oxygen, and zinc content. The P-Z-C bio-nanocomposite has also showed significant antimicrobial activity, with maximum antibacterial activity against *Escherichia coli* (20.133 mm inhibition zone at 20 ppm) and antifungal activity against *Aspergillus awamori* (15.433 mm inhibition zone). Moong beans (*Vigna radiata*) and mustard (*Brassica juncea*) seed germination and seedling growth were observed by dipping the seeds in the gel of bio-nanocomposite. The findings have shown the high potential of the composite for biomedical application, active food packaging, and agricultural nanoencapsulation. The research highlights the potential of biodegradable nanocomposite synthesized from renewable resource to mitigate the sustainability issues while imparting reliable functional performance.

KEYWORDS: bio-nanocomposite, antibacterial activity, antifungal activity, seed germination, sustainability.

1. INTRODUCTION

Nanotechnology promises enormous potential in the 21st century, with significant recent uses in biotechnology. Advancements in nano-enabled technologies have dramatically improved the quality of life and sparked the creation of novel bio-nanocomposites, systems, and therapeutic platforms. Bio-nanocomposites are materials that contain elements of biological origin with at least one dimension within the range of nanoscale (1–100 nm). In most cases, these composites are made by mixing natural polymers (biopolymers) with inorganic nanomaterials, which creates a matrix with nanoentities reinforcing it. This is the structure that enhances mechanical properties like strength, stiffness, and toughness [Menossi *et al.,* 2021]. These materials possess various benefits, such as being cost-effective, highly available, easy to fabricate, low in density, optically transparent, with good rheological properties, better surface properties, and better flame resistance.

of homopolymers, which tend to exhibit poor mechanical behavior, poor strength, and poor biodegradability [Aravind *et al.,* 2022]. The intrinsic structural characteristics of biopolymers make it easy to create pellets at the nanoscale with different shapes and sizes, broadening their scope in the field of nanocomposite applications [Basavegowd and Baek, 2021]. Blending, especially using polyhydroxyalkanoates, is an effective way to improve the properties of biopolymers. This process avoids the shortcomings of single polymers and has been in the spotlight for enhancing the physical and mechanical characteristics of polyhydroxybutyrate. PHB can be mixed with other biopolymers like starch, cellulose, and lignin to create high-end PHB-based bio-nanocomposites [Tripathi *et al.,* 2021]. These new composites can be processed in various forms, such as particles, fibers, moldings, films, membranes, foams, and coatings, based on their purpose of application [Raza *et al.,* 2019]. The addition of nanomaterials like chitosan, montmorillonite, zinc oxide (ZnO), and silver nanoparticles improves the mechanical, barrier, and physicochemical characteristics of films and coatings made of biopolymers. The materials also possess useful attributes likewise antimicrobial and antioxidant capabilities [Devi *et al.,* 2021]. For instance, ZnO nanoparticles in PHB-ZnO-chitosan bio-nanocomposites have the ability to suppress bacterial growth by binding to microbial membranes, interfering with nutrient transport, and eventually inducing cell lysis [Alaredhey *et al.,* 2022]. ZnO provides various benefits to biodegradable matrices including antibacterial activity, UV protection, and photocatalytic activity. The ROS formation, Zn^{2+} ion release, and UV light absorption properties of ZnO play a role in decreasing microbial growth and oxidation [Nahar and Sarker, 2026]. Chitosan exhibits antibacterial activity against *Escherichia coli* (*E. coli*) and *Staphylococcus aureus* (*S. aureus*) owing to electrostatic interactions between its polycationic chains and the negatively charged elements of bacterial cell surfaces. This interaction interferes with cell wall and membrane integrity, causing bacterial cell death [Dumont *et al.,* 2018]. There is a critical need to create biodegradable bio-nanocomposites from renewable biopolymers for various applications. Applications of biocomposites should extend beyond packaging materials to include the creation of biosensors that can promptly detect the presence of germs, contaminated food, and other issues. (Sharma *et al.,* 2022). Some of these applications are targeted drug delivery in the biomedical sciences, nanoencapsulation of agrochemicals in agriculture, and functional coatings for food packaging.

Recently, nano-agricultural methods brought NPs into agriculture because of their prospective applications in plants [Al-Dossary et al., 2025; Zhang et al., 2026]. The large surface-to-volume ratio of NPs, a consequence of their minute size relative to bulk materials, reduces the energy and raw material requirements needed to fabricate useful and valuable machines [Ghanaim *et al.,* 2025]. Numerous scientists have found that nanoparticles possess a better capacity to increase the rate of germination in plants [Deepa *et al.,* 2022]. Therefore, NPs impact the nutritional quality of seeds compared to control centers. Various nanoparticles as well as nanocomposites are utilized to boost the rate of germination as well as the growth of different plants by enhancing the absorption of light [Deepa *et al.,* 2023]. Since nanoparticles possess an increased large surface area and tiny dimensions, their biological and chemical activity is enhanced. Nanoparticles adsorb at the surface of macromolecules when they come into contact with tissues and fluids, then interact and have an impact on how proteins and enzymes are controlled [Danish *et al.,* 2025].

The smaller-sized metallic nanoparticles also enhance the generation of reactive oxygen species (ROS) with free radicals in metal oxide nanoparticles that exert significant effects on germination rate [Khan and Khan., 2023; Yusefi-Tanha *et al.,* 2024]. Researchers are quite concerned about the various health and environmental problems that nanoparticles have caused in recent years. However, nanotechnological techniques are indicating that NPs have harmful impacts on plants. Recently, a new route for controlled release systems has been made possible by nanotechnology. Recent developments in doped and green synthesized ZnO have resulted in increased oxidative stability in biodegradable materials [Jahani & Biglari, 2025].

The concept of slow release state as the regulation of releasing the effective substance into the targeted area from the engineered storage device, thereby guaranteeing that the concentration of the effective constituent remains at a desired stage for an interminable duration. Researchers have come up with many forms of nanocomposites with the ability to disperse agrochemicals, and owing to their high stability and longevity, the products provide an extensive product longevity that makes them especially appropriate for practical use in agriculture [Khan & Khan, 2023].

Although many studies have been done on the methods for the formation of nanocomposites, their physicochemical properties and the process of their degradation in agricultural settings such as soil and water bodies [Guha *et al.,* 2020].However, limited studies have been investigated the effects of the direct use of these

compounds in agriculture and the impact of their application on the plant growth and development [Dhanker *et al.,* 2021] Some preliminary laboratory studies have shown that the use of nanocomposites can improve the process of plant growth and development [Deepa *et al.,* 2022]. Hence, in this context, the current study aimed to evaluate the effect of nanocomposites on the growth rate of moong beans (*Vigna radiata*) and mustard (*Brassica juncea*).

2. MATERIALS AND METHODS

2.1. Preparation of PHB-Zinc-Chitosan Bio-nanocomposite

A simple precipitation technique was used for the preparation of PHB-zinc-chitosan nanocomposite [Revathi and Thambidurai, 2019]. First, 25 ml of 4% acetic acid solution was used for dissolving 0.45 g of PHB, with continuous stirring for 30 minutes. This solution was continuously stirred at 100°C with addition of 25 ml of the chitosan nanoparticle solution (3%) for 3 hours. Then, 25 ml of 0.5 M zinc oxide nanoparticles were added to the solution, and stirring was carried out for 2 hours at 80°C. Finally, 40 ml of 1M NaOH solution was added gradually to the solution to produce a precipitate. The resulting precipitation was allowed to stand for 24 hrs. The supernatant solution was then discarded, and the precipitation was washed multiple times with distilled water. Finally, the bio-nanocomposite was prepared by drying the precipitate at 100°C for 5 hrs.

2.2. Characterization of PHB-Zinc-Chitosan Bio-Nanocomposite

The prepared Polyhydroxybutyrate-Zinc-Chitosan (PHB-Z-C) bio-nanocomposite was characterized using Particle size analyser (PSA), Fourier Transform Infrared Spectroscopy (FTIR) spectra, and Field Emission Scanning Electron Microscope (FE-SEM) to study the size, functional groups, morphological, and elemental composition present in the samples.

In the study, the prepared bio-nanocomposite Polyhydroxybutyrate-Zinc-Chitosan (PHB-Z-C), had its functional groups by FTIR spectroscopy. The FTIR analysis was conducted under specific conditions, with a spectral range of 4000-400 cm^{-1} selected to accurately confirm the identification of functional groups in the extracted polymer. The FTIR spectra of PHB-zinc-chitosan bio-nanocomposite were recorded as pellets of potassium bromide (KBr). The particle size of synthesized bio-nanocomposite (PHB-Zinc-Chitosan) was measured by laser light scattering using Malvern Zetasizer Nano ZS90 (Department of Biochemistry, CCSHAU Hisar) based on quasi-elastic light scattering. The FE-SEM (JEOL IT800, Center for Nanobiotechnology, CCSHAU, Hisar) analysis was conducted using an accelerating voltage of 30 kV. For this purpose, a dried sample weighing 0.01 g was positioned on a stub coated with carbon tape and platinum coating and observed under the microscope.

Additionally, to determine the elemental composition in terms of atomic percentage and weight on the surface of the synthesized bio nanocomposite, Energy Dispersive X-ray Spectroscopy (EDX) was also carried out. X-ray diffraction was used to observe the crystalline nature of P-Z-C bio-nanocomposite samples. X-ray diffraction was done with Cu-Kα radiation (λ = 1.54 A°) in the range of 2θ = 2–30° [Pradhan *et al.,* 2018]. Graphs were plotted with intensity versus 2θ using Origin Pro 9.0 software.

2.3. Preparation of stock solution of bio-nanocomposite for antimicrobial evaluation

To prepare the bio-nanocomposite stock solution, ten milligrams of dried bio-nanocomposite powder (PHB-Zinc-Chitosan) were dissolved in 100 ml of sterile distilled water, resulting in a concentration of 100 ppm. The suspension was subjected to sonication at 25°C for 20 minutes to prevent aggregation and ensure thorough mixing of the solution. Subsequently, the suspension was autoclaved at 121°C for 20 minutes. Working concentrations of 0, 5, 10, and 20 ppm were prepared from the stock solution and were also sonicated for an additional 20 minutes before use.

2.4. Determination of antibacterial and antifungal activity of PHB-Zinc-Chitosan bio-nanocomposite

The agar diffusion assay was utilized to investigate the antibacterial and antifungal properties of bio-nanocomposite [[Revathi and Thambidurai, 2019; Munoz-Bonilla *et al.,* 2019]. Fresh subcultured bacterial and fungal cultures were used for this purpose. Separate evaluations were conducted for each bacterium (*Pseudomonas aeruginosa* ZSC6 OQ547421*, Bacillus cereus* VTCCBAA443 and (*Escherichia coli* VTCCBAA129) and fungus (*Fusarium oxysporum* and *Aspergillus awamori*) by amending nutrient agar and potato dextrose agar (PDA) plates with different concentrations of the bio nanocomposite, including 0 ppm, 5 ppm, 10 ppm, and 20 ppm. The sterilized filter paper discs were then carefully placed on the surface of the medium which was earlier inoculated with the test organism. The petri plates were incubated in an incubator to allow for confluent growth. The zones of inhibition formed around the discs were measured and recorded in millimeters (mm).

2.5. Seed germination assay of PHB-Zinc-Chitosan bio-nanocomposite

Germination of moong bean (*Vigna radiate)* and mustard seeds (*Brassica juncea*) was carried out by the dipping method. It was utilized to make a bio-nanocomposite gel PHB-Z-C when polyhydroxybutyrate was combined with zinc and chitosan under regulated conditions. The biocomposite gel serves as a biocompatible and biodegradable nutrient-rich and antimicrobial scaffold for various plants and produces a suitable environment for healthy seedlings. Twenty-four moong bean (*Vigna radiate)* and mustard seeds (*Brassica juncea*) were procured and were surface sterilized, then soaked in PHB9 (PHB9 was polyhydroxybutyrate extracted from strain *Bacillus velezensis* strain PHB9 (OQ600718.1)) used as a control and P-Z-C gel formulations. The P-Z-C bio-nanocomposite powder was used to make the gel formulation through a 1:10 ratio of glycerol with stirring to form

a slightly solid gel. Glycerol served as a solvent medium and a plasticizer that aided bio-nanocomposite dispersion and enhanced the mechanical flexibility and stability of the gel matrix. This dipping technique gives uniform coating to enable direct contact between the seed surface and bioactive compounds of the gel, leading to increase in bioavailability of different elements in the germination phase. Afterward, gel-dipped treated seeds were moved to petri dishes and placed inside a plant growth chamber that was set at 25 ± 2°C for 7 days. To assess the efficacy of bio-nanocomposite gel treatment, germination rate and seedling growth were monitored.

2.6. Statistical analysis

Three replicates were taken for the experiment and the results have been shown as mean ± SD. Statistical analysis was performed by Duncan's multiple range test at 0.05 probability level (95%). Means followed by different letters are statistically significant.

3. RESULTS AND DISCUSSION

3.1. Preparation of PHB-Zinc-Chitosan Bio-nanocomposite

The dried final form of the nanocomposite, which was created by combining chitosan, zinc oxide nanoparticles, and polyhydroxybutyrate (PHB), is an off-white powder. Zinc oxide's antibacterial action, chitosan's bioadhesive and film-forming qualities, and PHB's biodegradability and mechanical strength all work in collaboration to bring the product better qualities.

3.2. Fourier Transform Infra-Red (FTIR) Spectroscopy of PHB-Zinc-Chitosan Bio-nanocomposite

The FTIR spectra of PHB-Zinc Oxide-Chitosan (P-Z-C) bio-nanocomposite and nanoparticles, i.e., zinc oxide and chitosan, were recorded (**Fig. 1**). In the PHB-Zinc-Chitosan bio-nanocomposite, the absorption peak at 3444.88 cm^{-1} denoted OH (hydroxyl) group vibrations associated with strong hydrogen stretching. The C=O (carbonyl) functional group vibrations appeared at 1634.49 cm^{-1}. Additionally, an absorption peak at 2345.96 cm^{-1} indicated the appearance of aromatic C-H stretching vibrations, potentially suggesting interactions between the components in the bio-nanocomposite. The absorption band that appeared at 1567.66 cm^{-1} was said to be associated with the bending vibrations of N-H bonds, which may have suggested some changes in the nitrogen-containing functional groups of the material. In addition, the characteristic absorption band which visualized at 1052 cm^{-1} was due to the C-O stretching vibration. This signified the presence of functional groups that included the C-O bond, which can be attributed to compounds like alcohols, ethers, or esters. Prokhorov et al. (2020) studied CS-ZnO films and observed shifts in the absorption peaks of chitosan (CS) compared to CS-ZnO bio-nanocomposite. The shifts were evident at 1653 cm^{-1} for the amide group, 1555 cm^{-1} for NH_3 bending, and 1050 cm^{-1} for C-O-C linkages. However, chitosan (CS) at 1636 cm^{-1} (amide I group), 1542 cm^{-1} (NH_3 bending vibrations), and 1065 cm^{-1} (C–O–C stretching of glycosidic linkage). According to similar findings, the asymmetric and symmetric stretching vibration of -CH caused the peaks in the adsorption band 3000–2850 cm^{-1} to be seen for all kinds of peaks. All of the spectra had peaks at 1745 cm^{-1} and 1450 cm^{-1}, which were caused by the asymmetric bending vibrations of $–CH_3$ and the stretching vibrations of carbonyl groups (C=O), respectively. The distribution of carbonyl groups in the crystalline and amorphous areas of the nanocomposite filaments is greatly impacted by the zinc reinforcement. According to transmittance peaks, FTIR research unequivocally demonstrates that adding zinc to the PHB matrix results in observable alterations in the chemical structure [Trivedi and Gupta, 2024; Krzykowska *et al.,* 2024; Şen *et al.,* 2026]. PHB/CWR biocomposites analysis by FT-IR revealed some peak shifts that implied very weak intermolecular interaction or hydrogen bonding. The modifications in PHB peak indicated some changes in crystallinity. The presence of PHB methyl and methylene groups was suggested by peaks at 2935 and 2975 cm^{-1} [Ladhari *et al.,* 2025].

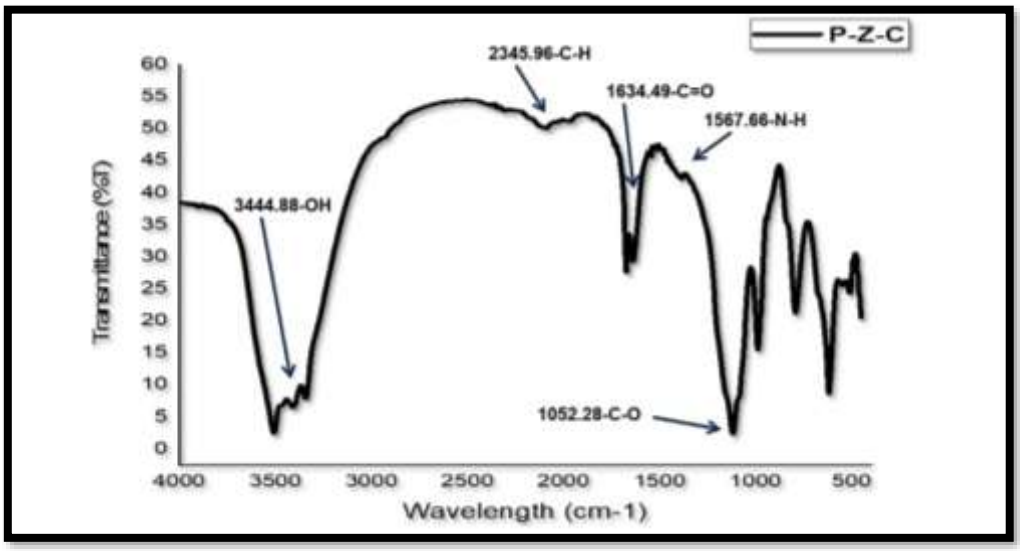

Fig. 1 FTIR spectrum of PHB-Zinc-Chitosan bio-nanocomposite

3.3. Particle size analyzer (PSA) of PHB-Zinc Oxide-Chitosan Bio-nanocomposite

The size of the bio-nanocomposite was measured by particle size analyzer, and their polydispersity indexes (PDI) were characterized by using a Malvern Zeta sizer Nano ZS90 based on quasi-elastic light scattering. The size and polydispersity index of synthesized bio-nanocomposite PHB-Zinc Chitosan was 104.1 nm in diameter (**Fig. 2**). Similar findings showed that the extracted PHB-silver nanocomposite had an average particle size of 23.6 nm and a PI index of 0.981 [Jayakumar *et al.,* 2020]. The smaller particle size and better distribution increase the effective surface area, which in turn allows for stronger interfacial interactions, better Zn^{2+} ion diffusion, and contact with biological systems, thereby contributing to the observed antimicrobial and biological performances [Sidhu *et al.,* 2025].

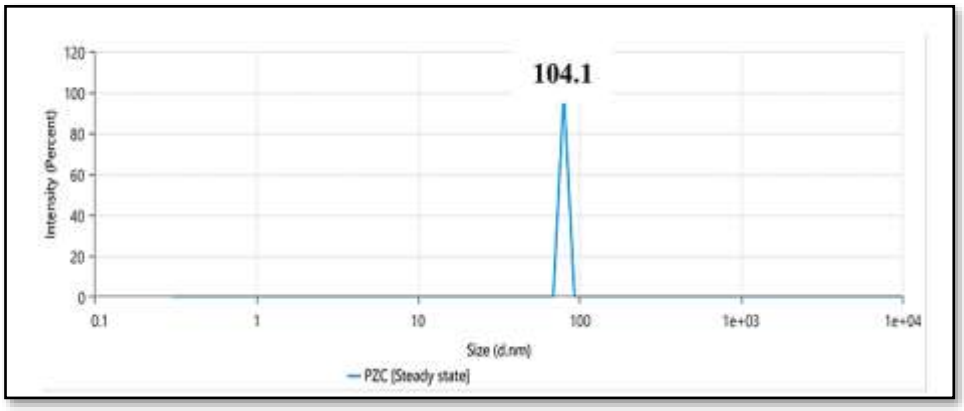

Fig. 2 Particle size analyzer of PHB-Zinc-Chitosan bio-nanocomposite.

3.4. X-Ray Diffraction of PHB-Zinc-Chitosan Bio-nanocomposite

The crystalline nature of the PHB-Zinc-Chitosan bio-nanocomposite was studied by X-ray diffraction (**Fig. 3**). The XRD pattern showed the major diffraction peaks at 8.4°, 10°, and 11°, which reflect orthorhombic unit cell structures of bio-nanocomposites. Moreover, secondary peaks were observed at 19°, 22.8°, 24°, and 30°, implying the existence of other crystalline phases. Similar results were reported that diffraction peaks at 35.86° and 53.02° were related to monoclinic CuO. In addition, the introduction of chitosan (CS) and nanocomposites was related to the decreased strength of the crystalline peaks, suggesting partial disruption or alteration of the crystalline structure in the CS-CuO nanocomposite [Revathi and Thambidurai, 2019; Jayakumar *et al.,* 2020]. While this confirms strong interfacial interactions among PHB, chitosan, and ZnO nanoparticles using XRD analysis, diminished crystallinity in PHB increases the flexibility of its chains, improving ion diffusion [Jayakumar *et al.,* 2020]. The XRD pattern of PHB-coHCS copolymers had some new peaks at certain points. These points were 2θ which was 9.3°, 30.64 ° and 35°. This meant that PHB-co-HCS copolymers formed a crystalline phase. It also meant that the PHB-co-HCS copolymers were successfully combined with PHB and CS [Sidhu *et al.,* 2025]. This suggests that in addition to the main α-crystals with helical chain shape in PHB, there are also some orthorhombic β-crystals with a zigzag configuration. The development of β-crystals indicates increased molecular stress in the amorphous regions around the α-lamellae [Salahuddin *et al.,* 2026]. The presence of diffraction peaks specific to ZnO, of reduced intensity, speaks for crystalline stability and homogeneity in its dispersion. These altogether present an enhanced biological performance [Imren *et al.,* 2026; Ibrahim *et al.,* 2022].

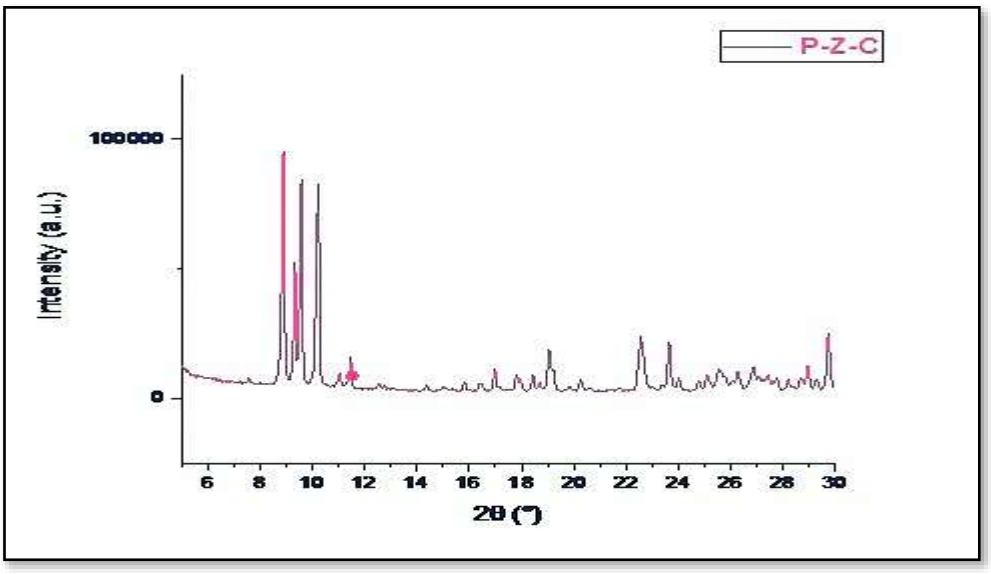

Fig. 3 X-Ray Diffraction of PHB-Zinc-Chitosan Bio-nanocomposite.

3.4. Field Emission-Surface Electron Microscopy (FE-SEM) of Bio-nanocomposite

Scanning Electron Microscopy (SEM) was used to analyze the surface morphology of the synthesized bio-nanocomposite. The SEM results revealed that the surface was rough and zinc clusters were embedded within the biopolymer matrix (**Fig. 4**). This indicated the successful incorporation of zinc into the bio-nanocomposite structure and ranged from 25 to 51.8 nm with a mean diameter of 32.4 nm.

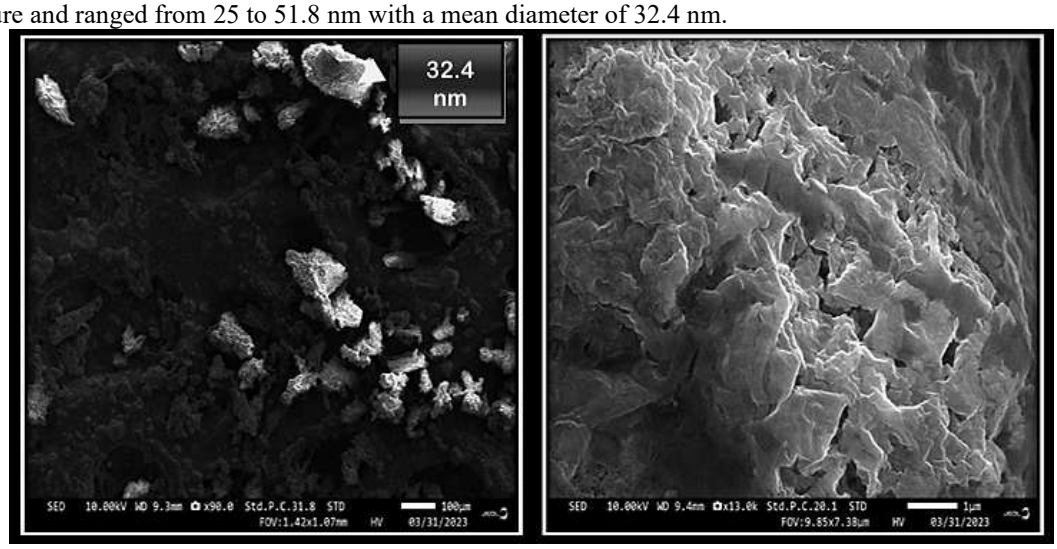

Fig. 4 Surface morphology of PHB-Zinc-Chitosan bio-nanocomposite.

Furthermore, Energy Dispersive X-ray Spectroscopy (EDX) analysis was done to investigate the elemental composition present on the surface of the synthesized bio-nanocomposite. By analyzing the X-ray signals emitted from the sample, the elemental composition, including the presence of zinc, could be identified and quantified (**Fig. 5**). The bio-nanocomposite contained 8.7% zinc, while carbon and oxygen constituted 35.6% and 36.5%, respectively. These proportions of carbon and oxygen offered structural support to both the PHB and chitosan components. Researchers revealed spherical-like particles of chitosan nanoparticles, and energy dispersive spectroscopy confirmed the presence of carbon and oxygen, representing the main elements of chitosan [Ali *et al.,* 2024]. The ZnO/polyhydroxybutyrate composites had a uniform distribution of irregular, micro-sized pores that were almost spherical throughout their whole surface [Trivedi *et al.,* 2024].

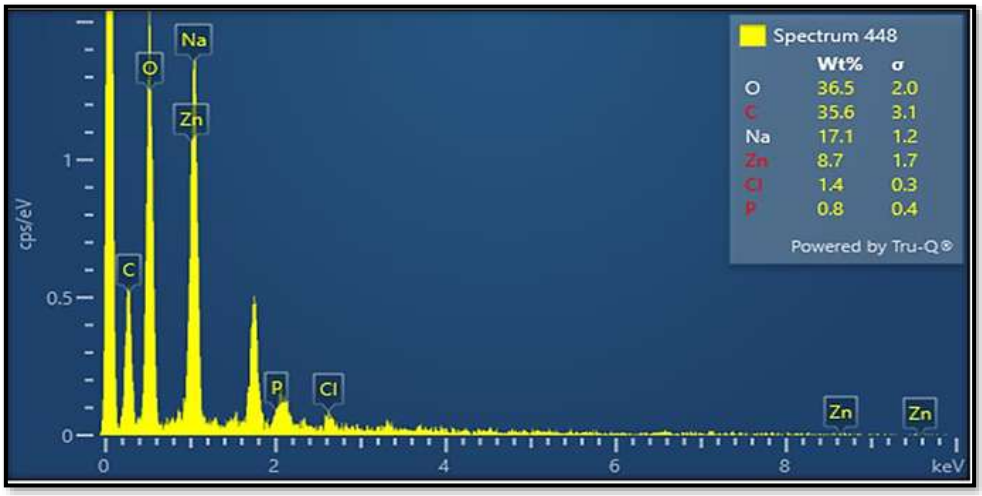

Fig. 5 Energy-dispersive X-ray spectroscopy of PHB-Zinc-Chitosan bio-nanocomposite.

3.6. Evaluation of Bio-nanocomposite for Antibacterial Activity Against Pathogenic Bacteria

The synthesized bio-nanocomposite (P-Z-C) was assessed for antibacterial activity against Gram-positive bacterium *Bacillus cereus* VTCCBAA443 and Gram-negative bacteria *Escherichia coli* VTCCBAA129 and *Pseudomonas aeruginosa* ZSC6 OQ547421 (**Table 1**). The antibacterial activity was determined by measuring the clearance zone around the sterilized filter paper disc in a zone of inhibition test. The size of the clearance zone varied among the bacteria, with the highest inhibition observed against *E. coli* (20.13 mm) at 20 ppm concentration as compared to 10 ppm (**Fig. 6**). The antibacterial effect of PHB-ZnO bio-nanocomposites, which were tested against *Escherichia coli* and *Staphylococcus aureus*. The highest antibacterial activity, 98% and 95% growth inhibition for *E. coli* and *S. aureus,* is observed at 5.0 wt% ZnO loading [El-Naggar *et al.,* 2022]. The nanoparticles in nanocomposite induce the production of ROS, causing the destruction of bacterial cells and causing lipid peroxidation, which disrupts membrane integrity and leads to cell death [Díez-Pascual, 2022]. The improved antimicrobial efficacy of the PHB-Zn-Chitosan nanocomposite is attributed to the combined effects of Zn^{2+} ion release, chitosan-mediated membrane interaction, and nanoscale dispersibility in the polymeric matrix. The relatively improved antimicrobial efficacy against *E. coli* compared to that in *B. cereus* can be led by the

negatively charged outer membrane of Gram-negative bacteria that enhanced electrostatic interactions with Zn^{2+} ions as well as protonated chitosan, thus causing enhanced membrane permeability and cellular destruction [El-Naggar *et al.,* 2022]. Hence, the antibacterial activity demonstrated in the present investigation reveals that ZnO-mediated mechanisms in the nanocomposite play a major role instead of chitosan itself being the active component.

Table 1. Antibacterial activity of PHB-Zinc-Chitosan (P-Z-C) bio-nanocomposite and PHB9 against pathogenic bacteria.

Pathogenic bacteria	**Bio-nanocomposite (ppm)**	**Zone of inhibition (mm)**
Escherichia coli VTCCBAA129	P-Z-C (10 ppm)	7.00 ± 0.3^{g}
	P-Z-C (20 ppm)	20.13 ± 1.5^{a}
Bacillus cereus VTCCBAA443	P-Z-C (10 ppm)	13.70 ± 1.4^{e}
	P-Z-C (20 ppm)	15.33 ± 1.4^{d}
	PHB 9	10.00 ± 1.2^{c}
Pseudomonas aeruginosa ZSC6 OQ547421	P-Z-C (10 ppm)	9.83 ± 1.3^{g}
	P-Z-C (20 ppm)	17.83 ± 1.3^{f}
	PHB9	5.30 ± 1.4^{b}

The data are reported as mean values ± standard deviations (SD). Mean values with different letters represent statistically significant differences at $p < 0.05$, 95% confidence level, according to Duncan's multiple range test.

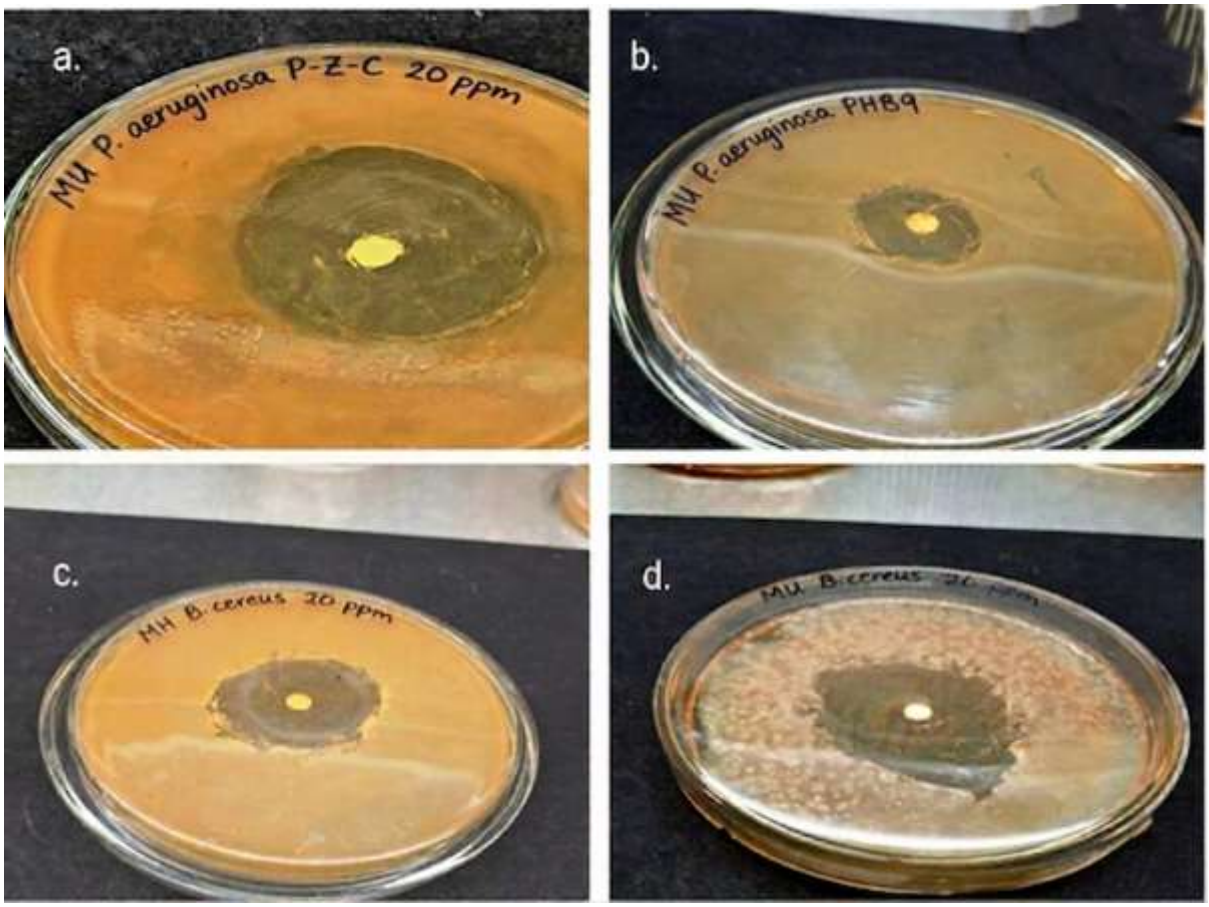

Fig. 6 Bio-nanocomposite (P-Z-C) and PHB9 show inhibition zones against (a, b) *P. aeruginosa*, (c) *B. cereus,* and (d) *E. coli.*

3.8. Evaluation of Bio-nanocomposite for Antifungal Activity Against Pathogenic Fungi

The synthesized bio-nanocomposite (P-Z-C) was assessed for antifungal activity against the pathogenic fungi *Aspergillus awamori* and *Fusarium oxysporum* (Table 2). The antifungal activity was investigated by measuring the clearance zone around the sterilized filter paper disc in a zone of inhibition test. The size of the clearance zone varied among the fungi, with the highest inhibition observed against *Aspergillus awamori* (15.43 mm), followed by *Fusarium oxysporum* (7.33 mm) at 20 ppm concentration (**Fig. 7**). Similar studies observed the antifungal activity of bio nanocomposites (PHB-TPS-OMMT) with and without eugenol against *Botrytis cinerea, which* was assessed by measuring the area of inhibition. Increasing eugenol concentrations in the bio nanocomposites led to significant growth reductions, with the greatest inhibition area observed at 6.4 ± 2.5 cm (with 2% eugenol) [Safari *et al.,* 2025]. Eugenol's fungicide mechanism induces morphological anomalies that hinder the fungus' growth by attacking its membrane and cell wall, interfering with ergosterol biosynthesis, and disrupting the membrane's integrity and functionality [Garrido-Miranda *et al.,* 2018].

Table 2. Antifungal activity of PHB-Zinc-Chitosan (P-Z-C) biocomposite against pathogenic fungus.

Pathogenic fungus	Bio-nanocomposite (ppm)	Zone of inhibition (mm)
Aspergillus awamori	P-Z-C (5 ppm)	4.60 ± 0.4^{d}
	P-Z-C (10 ppm)	7.13 ± 0.2^{b}
	P-Z-C (20 ppm)	15.43 ± 0.5^{a}
Fusarium oxysporum	P-Z-C (5 ppm)	3.50 ± 0.4^{e}
	P-Z-C (10 ppm)	6.16 ± 0.6^{c}
	P-Z-C (20 ppm)	$7.33\ \pm0.6^{b}$

The data are reported as mean values ± standard deviations (SD). Mean values with different letters represent statistically significant differences at $p < 0.05$, 95% confidence level, according to Duncan's multiple range test.

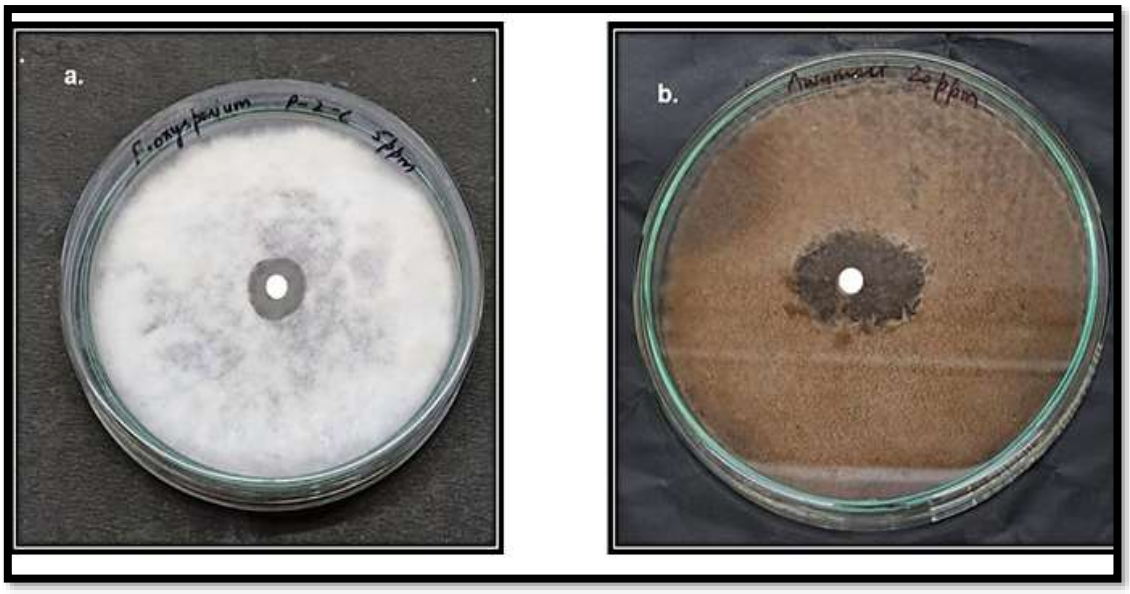

Fig. 7 P-Z-C shows the inhibition zone against (a) *Fusarium oxysporum* and (b) *Aspergillus awamori* using the disc diffusion method.

3.9. Effect of PHB-Zinc-Chitosan Bio-nanocomposite on Seed Germination Assay

The seed germination test was done to test the potential of the PHB-Zinc-Chitosan (P-Z-C) bio-nanocomposite gel to enhance seed germination and seedling growth of moong bean (*Vigna radiate)* and mustard seeds (*Brassica juncea*) (**Fig. 8**). Seeds were subjected to PHB9 as a control and P-Z-C bio-nanocomposite gel and incubated in a plant growth chamber for 7 days. The treatment with P-Z-C bio-nanocomposite gel had a positive impact on seed germination and seedling growth, especially in moong beans. Germination percentage was elevated from 62% to 75% in moong and from 25% to 50% in mustard seeds after treatment with the bio-nanocomposite gel, as against the PHB9 control (**Table 3**). Radicle and plumule elongation also increased substantially. Moong seedlings treated with P-Z-C gel had radicles (4.2 cm) and plumules (13.5 cm) longer than those treated with PHB9 alone. This

enhancement is presumably due to the gel's biocompatibility and nutrient-dense nature. Zinc and chitosan, the substances present in the gel, are both known to affect plant growth through regulation of enzymatic activity and enhanced nutrient uptake. These results align with previous research findings that nanoparticles increase germination by leading to increased uptake of water, enhanced nutrient uptake, and triggering positive biochemical alterations such as high levels of production of reactive oxygen species. The uniform coating obtained through the dipping process must have enabled enhanced bioavailability of bioactive compounds at an early development stage of the seedling [Patyal *et al.,* 2025]. Enhanced seed germination is made possible by the controlled availability of zinc, a crucial micronutrient that activates enzymes and participates in the early processes of plant metabolism. The PHB-chitosan carrier probably controls the release of Zn^{2+} while increasing the water uptake, hence contributing to germination rather than toxicity [Chouhan *et al.,* 2025].

Fig. 8 PHB-Zinc-Chitosan (P-Z-C) bio-nanocomposite gel and PHB9 effect on seed germination.

Table 3. Effect of PHB-Zinc-Chitosan Bio-nanocomposite Gel on Seed Germination

Seeds	No. of seeds germinated	Radicle length (cm)	Plumule length (cm)	Cotyledon length (cm)	Germination (%)
Mustard Gel	4/8	2.9 ± 0.01^{c}	5.5 ± 0.1^{c}	0.5 ± 0.01^{b}	50 ± 0.5^{c}
Mustard PHB9	2/8	1.7 ± 0.01^{d}	6.0 ± 0.1^{c}	0.2 ± 0.01^{b}	25 ± 0.6^{d}
Moong Gel	6/8	4.2 ± 0.02^{a}	13.5 ± 0.2^{a}	2.0 ± 0.01^{a}	75 ± 1.0^{a}
Moong PHB9	5/8	3.4 ± 0.02^{b}	10.5 ± 0.2^{b}	1.7 ± 0.01^{a}	62 ± 1.0^{b}

The data are reported as mean values ± standard deviations (SD). Mean values with different letters represent statistically significant differences at $p < 0.05$, 95% confidence level, according to Duncan's multiple range test.

CONCLUSION

There is currently interest in research on bio-based nanocomposites in an attempt to build a more environmentally friendly, sustainable world. While many metallic nanoparticles can be used to create PHB bionanocomposites, their high aspect ratio and natural character make them stand out. Using a simple precipitation technique, PHB9 was combined with zinc and chitosan nanoparticles, resulting in PHB-based bio-nanocomposites with a diameter of 104.1 nm. Additionally, the FTIR and XRD examinations demonstrated the presence of functional groups and the crystalline nature of bio-nanocomposites. Scanning electron microscopy (SEM) demonstrated the unique material's porous surface. The inhibition zone of PHB-Zinc-Chitosan bio-nanocomposite (20 ppm) against *Escherichia coli* VTCCBAA129 was 20.13 mm, while the inhibition zone of PHB9 against *Pseudomonas aeruginosa* ZSC6 was 5.30 mm. At various concentrations of 5 ppm, 10 ppm, and 20 ppm, the antifungal capabilities of PHB-Zinc-Chitosan bio-nanocomposite against fungal infections were evaluated for *F. oxysporum* and *Aspergillus awamori*. At 20 parts per million, the highest zone of inhibition against *A. awamori* was 15.433 mm. Following the antimicrobial activity evaluation, a seed germination test was carried out to estimate the viability of the PHB-Zinc-Chitosan (P-Z-C) bio-nanocomposite in enhancing the growth of moong bean (*Vigna radiate)* and mustard seeds (*Brassica juncea*). P-Z-C bio-nanocomposite gel treatment provided a remarkable

positive influence on seed germination and seedling development, particularly for moong beans. It was found that increased soaking duration at low concentrations of synthesized bio-nanocomposite decreases the germination percentage and root and shoot growth. The bionanocomposites produced are believed to be extremely fascinating for designing and developing biodegradable active packaging materials for food and the food industry in addition to agricultural nanoencapsulation. Because there is less information on nanomaterial-crop interactions, it is challenging to determine the quality of food products of nanofertilizer supplied crops. Therefore, for enhancing the acceptability of nanocomposites in agricultural applications, further elaborated studies on the safety of these nanocomposites to the environment and public health are needed.

AUTHOR CONTRIBUTION
Conceptualization, Kashish Sharma, Kamla Malik, Shivi Choudhary, writing—original draft preparation, Kashish Sharma, Kamla Malik, Shivi Choudhary, review and editing, Kashish Sharma, Kamla Malik, Raunak Dhanker, Shivi Choudhary, Sahreen Naseer, Sujeeta Yadav, Priyanka Sangwan, Shivani, Sudiksha Pathania; visualization and supervision, Kashish Sharma, Kamla Malik, Raunak Dhanker, Shivi Choudhary, Sahreen Naseer, Sujeeta Yadav, Priyanka Sangwan, Shivani, Sudiksha Pathania. All authors have read and agreed to the published version of the manuscript.

Data availability
The data supporting the findings of this study are available from the corresponding author upon reasonable request.

Funding
Not applicable

Data Availability
All data generated or analyzed during this study are included in this published article.

Code availability
Not applicable.

Declarations
Ethical Approval
Not applicable.

Research Involving Humans and Animals Statement
Not applicable.

Informed Consent
Not applicable.

Competing Interests
The authors declare no competing interests.

REFERENCES
1. Alaredhey, A. S., Al-janabi, D. R., and Al-luhaiby, A. I. (2022). Antibacterial activity of zinc oxide nanoparticles-poly-β-hydroxybutyrate bio-nanocomposites on *Staphylococcus* spp. *International Journal of Health Sciences*, 6(2):815–823.
2. Al-Dossary, O., Alnaddaf, L. M., and Al-Khayri, J. M. (2025). Crop management to enhance plant resilience to abiotic stress using nanotechnology: Towards more efficient and sustainable agriculture. *Frontiers in Plant Science,* 16, 1626624. https://doi.org/10.3389/fpls.2025.1626624
3. Ali, S., Dayo, M., Alahmadi, S., and Mohamed, A. (2024). Chitosan-supported ZnO nanoparticles: Their green synthesis, characterization, and application for the removal of pyridoxine HCl from aqueous media. *Molecules,* **29**(4): 828. https://doi.org/10.3390/molecules29040828
4. Aravind, D., Senthilkumar, K., Chandrasekar, M., Muthu Kumar, T. S., Ganesan, C., Parameswaranpillai, J., Rajini, N., Siengchin, S., & Varagunapandiyan, N. (2022). A compendious review on fatigue properties of the bio-nanocomposites. *Polymer Composites*, 43(10), 6803-6816. https://doi.org/10.1002/pc.26859
5. Basavegowda N, Baek K-H. (2021). Advances in Functional Biopolymer-Based Nanocomposites for Active Food Packaging Applications. *Polymers*. **13**(23):4198. https://doi.org/10.3390/polym13234198
6. Chouhan, D., Dutta, P., Dutta, D., et al. (2025). Effect of silver nanochitosan on control of seed-borne pathogens and maintaining seed quality of wheat. *Phytopathology Research,* **6**: 41. https://doi.org/10.1186/s42483-024-00260-x
7. Danish M, Shahid M, Farah MA, Al-Anazi KM, Ahmed SM, Mohamed HI, Ahamad L. (2025). CuO-ZnO nanocomposites mitigate root-knot nematode stress in Vigna radiata by enhancing physiological and antioxidant defense responses. *Physiological and Molecular Plant Pathology.*139:102776. https://doi.org/10.1016/j.pmpp.2025.102776

8. Deepa, Ameen, F., Islam, M. A., & Dhanker, R. (2022). Green synthesis of silver nanoparticles from vegetable waste of pea (Pisum sativum) and bottle gourd (Lagenaria siceraria): Characterization and antibacterial activity. Frontiers in Environmental Science, 10, 941554. https://doi.org/10.3389/fenvs.2022.941554
9. Deepa, Dhanker, R., Kumar, R., Kamble, S. S., Kamakshi, & Goyal, S. (2023). Biosynthesis and characterization of silver nanoparticles generated from peels of Solanum tuberosum (potato) and their antibacterial and wastewater treatment potential. Frontiers in Nanotechnology, 5, 1213160. https://doi.org/10.3389/fnano.2023.1213160
10. Devi, L.S., Purkayastha, M.D., Mukherjee, A., and Kumar, S. (2021) Biopolymer-based Films and Coatings: Emerging Technologies to Extend Shelf-life of Fruits and Vegetables. *Prayogik Rasayan* 5(3):82-91. https://doi.org/10.53023/p.rasayan-20211211
11. Dhanker, R., Hussain, T., Tyagi, P., Singh, K. J., & Kamble, S. S. (2021). The emerging trend of bio-engineering approaches for microbial nanomaterial synthesis and its applications. Frontiers in Microbiology, 12, 638003. https://doi.org/10.3389/fmicb.2021.638003
12. Díez-Pascual, A. M. (2022). Poly (3-hydroxybutyrate-co-3-hydroxyhexanoate) with zinc oxide nanoparticles for food packaging. *Journal of Food Process Engineering,* 45(7): e13814.
13. Dumont, M., Villet, R., Guirand, M., Montembault, A., Delair, T., Lack, S. and David, L. (2018). Processing and antibacterial properties of chitosan-coated alginate fibers. *Carbohydrate polymers*, 190:31-42.
14. El-Naggar, N. E. A., Shiha, A. M., Mahrous, H. and Mohammed, A. A. (2022). Green synthesis of chitosan nanoparticles, optimization, characterization and antibacterial efficacy against multi drug resistant biofilm-forming *Acinetobacter baumannii. Scientific Reports,* 12(1):19869.
15. Garrido-Miranda, K. A., Rivas, B. L., Perez-Rivera, M. A., Sanfuentes, E. A. and Pena-Farfal, C. (2018). Antioxidant and antifungal effects of eugenol incorporated in bio-nanocomposites of poly (3-hydroxybutyrate)-thermoplastic starch. *LWT-Food Science and Technology,* 98:260-267.
16. Ghanaim AM, Mahmoud GA, Mohamed HI, Hanafy RS, Zaki LM, Mahmoud M, Mogazy AM. (2025). *Bacillus subtilis* and chitosan nanoparticles enhance potato virus Y (PVY) tolerance in tomato (Solanum lycopersicum L.) via modulation of antioxidants and secondary metabolites. *BMC plant biology*. 25(1):1613. https://doi.org/10.1186/s12870-025-07617-0
17. Guha, T., Gopal, G., Kundu, R., and Mukherjee, A. (2020). Nanocomposites for delivering agrochemicals: A comprehensive review. *Journal of Agricultural and Food Chemistry*, *68*(12): 3691-3702.
18. Ibrahim, M. I., Alsafadi, D., Alamry, K. A., Oves, M., Alosaimi, A. M., and Hussein, M. A. (2022). A promising antimicrobial bionanocomposite based poly (3-hydroxybutyrate-co-3-hydroxyvalerate) reinforced silver doped zinc oxide nanoparticles. *Scientific Reports*, 12(1): 14299.
19. Imren, E., Kocatürk, E., Şen, F., Zor, M., Özlüsoylu, Ş., Özgürlük, Ö., & Aydemir, D. (2026). Eco-Friendly Polyhydroxybutyrate Composite Films Reinforced with Cellulose and Holocellulose Fibers by the Solvent Casting. *Polymers,* **18**(8): 997. https://doi.org/10.3390/polym18080997
20. Jahani, A., & Biglari, N. (2025). Zinc oxide nanoparticles: synthesis, properties and their applications in food packaging. *Mater Chem Horiz*, **3**: 1076.
21. Jayakumar, A., Prabhu, K., Shah, L., and Radha, P. (2020). Biologically and environmentally benign approach for PHB-silver nanocomposite synthesis and its characterization. *Polymer Testing*, *81*: 106197.
22. Khan M.F. and Khan M.A. (2023). Plant-Derived Metal Nanoparticles (PDMNPs): Synthesis, Characterization, and Oxidative Stress-Mediated Therapeutic Actions. Future Pharmacology. 3(1):252-295. https://doi.org/10.3390/futurepharmacol3010018
23. Krzykowska, B., Uram, Ł., Frącz, W., Kovářová, M., Sedlařík, V., Hanusova, D., and Zarzyka, I. (2024). Polymer Bionanocomposites Based on a P3BH/Polyurethane Matrix with Organomodified Montmorillonite—Mechanical and Thermal Properties, Biodegradability, and Cytotoxicity. *Polymers*, 16(18): 2681.
24. Ladhari, S., Vu, N. N., Bastien, J. V., Tran, B. V., Nguyen, T. H., Saidi, A., and Nguyen Tri, P. (2025). A green synthesis route of ZnO/polyhydroxybutyrate composites with antibacterial and biodegradable properties. *Polymer Engineering and Science*, 65(3): 1037-1054.
25. Menossi, M., Cisneros, M., Alvarez, V.A. and Casalongue, C. (2021). Current and emerging biodegradable mulch films based on polysaccharide bio-composites. A review. *Agron. Sustain. Dev.,* 41:53.
26. Munoz-Bonilla, A., Echeverria, C., Sonseca, A., Arrieta, M. P. and Fernandez-Garcia, M. (2019). Bio-Based Polymers with Development. *Materials,* 12: 641.
27. Nahar, L., & Sarker, S. D. (2026). Active bio-packaging with PHBHHx-ZnO bionanocomposites: Advancing food safety and shelf-life. *Frontiers in Nutrition*, **13**: 1789448. https://doi.org/10.3389/fnut.2026.1789448
28. Patyal D, Sachdeva K, Sharma K, Khan RR. (2025). An innovative and sustainable seed coating technology for improving seed quality and crop performance. *J Sci Res Rep*., 31:597-607.
29. Pradhan, S., Dikshit, P. K., and Moholkar, V. S. (2018). Production, ultrasonic extraction, and characterization of poly (3-hydroxybutyrate) (PHB) using *Bacillus megaterium* and *Cupriavidus necator*. *Polymers for Advanced Technologies*, 29: 2392–2400.
30. Raza, Z. A., Noor, S. and Khalil, S. (2019) Recent developments in the synthesis of poly(hydroxybutyrate) based biocomposites. *Biotechnology Progress,* 2019: e2855.
31. Revathi, T., and Thambidurai, S. (2019). Cytotoxic, antioxidant and antibacterial activities of copper oxide incorporated chitosan-neem seed biocomposites. *International Journal of Biological Macromolecules, 139*: 867-878.

32. Safari, P., Rahimabadi, E.Z., Vaezi, M.R., *et al.* (2025). Development of ZnO-NPs reinforced chitosan nanofiber mats with improved antibacterial and biocompatibility properties. *Sci Rep* **15**: 16567 https://doi.org/10.1038/s41598-025-01669-w
33. Salahuddin, N., Gaber, M., Mousa, M. *et al.* (2026). Curcumin delivery system based on biodegradable polyhydroxybuterate Chitosan copolymer and Cobalt oxide nanoparticles against colorectal cancer. *Sci Rep* **16**, 8722. https://doi.org/10.1038/s41598-025-34587-y
34. Şen, F., Zor, M. and Candan, Z. (2026). Polyhydroxybutyrate/carbonized waste rubber biocomposite films. *Scientific Reports*, 16: 9703. https://doi.org/10.1038/s41598-026-45256-z.
35. Sharma, K., Malik, K., Choudhary, S., Kumar, S. *et al.* (2022). Polyhydroxybutyrates (PHBs): an eco-friendly alternative to petroleum-based plastics for diminution of their detrimental effects on the environment. *International Journal of Agricultural and Applied Sciences*, 3(2):8-18. https://doi.org/10.52804/ijaas2022.322
36. Sidhu, A.K., Verma, N., Kaushal, P. *et al.* (2025). Green synthesis of polymeric nanoparticles: agricultural applications and toxicological implications. *Discov Appl Sci* **7**: 505. https://doi.org/10.1007/s42452-025-06877-7
37. Tripathi, A. D., Paul, V., Agarwal, A., Sharma, R., Hashempour-Baltork, F., Rashidi, L. and Darani, K. (2021). Production of polyhydroxyalkanoates using dairy processing waste—a review. *Bioresour Technol.,* 326:124735.
38. Trivedi, A. K., and Gupta, M. K. (2024). PLA-based biodegradable bionanocomposite filaments reinforced with nanocellulose: development and analysis of properties. *Scientific Reports*, 14(1): 23819.
39. Yusefi-Tanha, E., Fallah, S., Pokhrel, L.R. et al. (2024). Role of particle size-dependent copper bioaccumulation-mediated oxidative stress on Glycine max (L.) yield parameters with soil-applied copper oxide nanoparticles. *Environ Sci Pollut Res*, 31: 28905–28921 https://doi.org/10.1007/s11356-024-33070-x
40. Zhang J, Zhang T, Rui Y. (2026) From Nanomaterials to Nanofertilizers: Applications, Ecological Risks, and Prospects for Sustainable Agriculture. *Plants*. 15(3):415. https://doi.org/10.3390/plants15030415